Reply to Reviewer #3

We thank the Reviewer for carefully reviewing our manuscript and providing insightful comments. Below we address each comment point by point. For clarity we mark the reviewer comment in **blue**, our answers in **black**, and changes to the manuscript in **red**. Page and line numbers in our replies refer to the revised manuscript.

In this work, Buchholz et al. demonstrated for the first time the application of positive matrix factorization (PMF) on high-resolution FIGAERO-CIMS data. They were able to identify distinct volatility classes, background, and decomposition products as PMF factors. Their results also offer additional confirmation of the effects of aerosol water on partitioning and particle-phase processes. Overall, the manuscript is well written and the approach described is novel. However, I have some concerns with the PMF design, experimental design, and data interpretation as described below. I would recommend the manuscript for publication in ACP if these comments are addressed.

PMF design and interpretation

2.3.1, page 7, line 19-22. The advantage of PMF is that it requires no a priori information. Pre-grouping thermograms based on knowledge about the SOA precursors, extent of aging, and aerosol water content defeats the purpose of using PMF, if not for laboratory sample then certainly for ambient samples. The advancement brought by the FIGAERO thermogram PMF in its current state is perhaps overstated. This limitation should be discussed in the manuscript. The analysis could also be carried out further to involve different SOA types all at once to validate its usefulness in a broader context.

This is the first study applying PMF analysis to FIGAERO-CIMS thermal desorption data. We had to prove that the splitting of single ion thermograms into multiple factors, especially at higher desorption temperatures, was not simply a mathematical construct to reduce Q/Qexp by just adding more factors. With the information about the prior isothermal evaporation (i.e. having samples where the volatile fraction of the particles was removed) we verified that with the removal of the more volatile fraction of the aerosol we removed the low temperature factors whereas the ones formerly explaining the "tail" of the single ion thermograms remained (as shown for three examples in Figure 8).

When applying PMF to a data set of FIGAERO-CIMS thermal desorption data (here all OC cases or generally, ambient data), there were two driving forces for the grouping of compounds into factors: their volatility and their "source" in the atmosphere/chamber/OFR (biomass burning, oxidation of different precursors, day-time/night-time chemistry, etc.). As we were more interested in identifying changes in the volatility due to the isothermal evaporation treatment, we decided to remove the influence of the different SOA sources (here the different oxidation regimes in the OFR) from the data set by splitting it into three groups. This was mostly done to highlight the particle phase processes and reduce the number of factors that had to be compared in each case (7 – 9 vs. 13 or more). The lower number of factors in each case also improves the overall clarity of

the manuscript. But pre-grouping the data is not a requirement for using PMF with thermal desorption data. We adjusted the last paragraph of section 2.3.1 to clarify this:

When performing PMF with the combined dataset with all available thermogram scans, the large number of factors (13 or more) necessary to explain the observed variability complicated the analysis and interpretation (see case study in SI section 1.4). Thus, the thermogram scans were grouped by SOA type (i.e., t_{evap} = 0.25 h & 4 h particles, dry & wet conditions of one SOA type: four thermogram scans per group). This pre-grouping reduced the number of factors in each group enhancing their interpretability while still enabling a direct investigation of the changes due to the evaporation/humidification for one SOA type. But generally, splitting the data by SOA type or even knowing about such different SOA types/sources in the data is not a requirement for analysing a thermogram dataset with PMF.

The information about using the filter blank data was moved to the description of the treatment of raw data in section 2.2 (page 4, line24):

For the PMF analysis, we did not subtract the filter blank measurements but rather added the corresponding filter blank thermograms to the dataset to help with the identification of the background factors, i.e., factors dominated by compounds from the instrument and/or filter background (more details on factor identification in section 3.1).

We strengthen this argument with the case study now provided in SI section 1.4 (see comment below) which concludes with:

This case study shows that the same overall conclusions can be drawn by pre-grouping the data according to the information of the sampling conditions (here the SOA type) or the combined dataset. With the combined dataset a higher number of factors (here at least 13) has to be chosen to cover all details in the dataset equally well. For ambient data a combined, dataset approach is favourable as limited information is available for any pre-grouping and such an extra step is not desirable. For a detailed study on e.g. particle phase processes with designed SOA types (as presented in this study), a pre-grouping can be beneficial to highlight the fine details hidden in the dataset.

We elaborate on comparing the different SOA types/running PMF on combined data sets in the reply to the next two comments and added two new section about this to the SI material (section 1.3 and 1.4).

3.1. Page 11, Line 10-13: Why is not a consistent factor identified across all SOA types (L, M, H, x dry, humid)? Is it expected that, for example, species that make up LV1 have negligible contributions to the overall SOA mass and evaporation behavior under the MediumOC ("M") conditions? It seems to me that there is significant factor blending here. Have the authors tried to combine the different SOA types (e.g. L and M) and see if the different factors (e.g. LV1, LV2, MV1, MV2) can be retrieved all the same?

We have combined different SOA types at the same sampling condition for PMF analysis. We present this investigation in the new SI section 1.4 and the summarised conclusions are presented in the reply to the next comment.

Page 12. Line 3 to 7: Filter/instrument-related background should be consistent for low- and mediumOC samples. The direct evaporation ions after isothermal evaporation observed in lowOC samples should therefore be expected to appear in the mediumOC sample as well, but why do they not?

This and the previous comment require a more detailed explanation of the performance of PMF for datasets with two different driving forces for the grouping into factors (here SOA type and volatility). As this explanation is also of interest to the future readers of our manuscript, we decided to add two new sections to the SI material. The SI sections are referred to in the manuscript in section 3.1 after the V-type factors are described (page 11 line 20). In SI section 1.3 (also see below) we use an artificial data set to inspect the way in which PMF groups compounds of the same volatility but with different contribution to the SOA samples. In section SI 1.4, we now present PMF results from a dataset combining all three SOA types (low-, medium-, and highOC) for one sampling condition (dry, t_{evap} = 4h). This sampling condition was chosen to remove the influence of the additional contamination (lowOC, dry, t_{evap} = 0.25h) and wet chemistry (highOC wet samples) which would introduce another 2 - 4 factors in the solution.

Briefly, although there are many ions in common especially for the low- and mediumOC case (as the reviewer also points out), this does not necessarily lead to common factors between the SOA types. The ratios between the ions changes significantly (i.e. a common ion A is associated with a set of compounds in one SOA type and correlates with another set of compounds in the other) as the oxidation chemistry is changed switching from low- to mediumOC SOA forming conditions in the OFR. This change in SOA source will dominate the grouping in PMF for compounds with similar volatility. This is what is meant at the end of the Conclusions by "A careful PMF analysis of the thermogram data will reveal the changes in volatility and the contribution of thermal decomposition to the signal in addition to information about changes in the physical sources of the organic material.".

Combining the different SOA types leads to a number of common factors if an 8-factor solution is selected. However, this solution would not be categorised as "best" according to the criteria used to select the solution for the pre-grouped dataset. A 13-factor solution (which is of the same quality as the ones for the pre-grouped dataset) explains 20-25% of the signal of each SOA type by common factors. All V-type factors from the pre-grouped dataset have a similar counterpart in the 13-factor solution. Thus, we conclude that the pre-grouping is not the main reason for the absence of common factors between the SOA types but caused by the reasons given in the previous paragraph and in more detail in SI section 1.3.

SI section 1.3:

1.3 Drivers controlling the grouping of compounds into PMF factors

When analysing a data set of FIGAERO-CIMS thermal desorption containing multiple samples with PMF, there are two driving forces for the grouping of compounds into factors: their volatility and their "source" in the atmosphere/chamber/OFR

(biomass burning, oxidation of different precursors, day-time/night-time chemistry, etc.). To investigate the competition between these two drivers, we create simple artificial data sets (Figure S 10). We combine 4 compounds A, B, C, and D (with nominal ion masses of 1, 2, 3, and 4) to form 4 SOA types (SOA1, SOA2, SOA3, SOA4). A, B, and C have the same volatility. A has the same thermogram in each SOA type.

In scenario X, we investigate as an extreme case the combination of SOA1 (containing A, B, and D) and SOA2 (containing A, C, and D). This scenario can be interpreted one source/process creating A and B at the same time for SOA1, but than a different pathway created A together with C in the case of SOA2. The 3-factor solution PMF result for this scenario (SOA1 & SOA2) is shown in Figure S 11. The common compound A has exactly the same thermogram behaviour in both samples. But as it once correlates with B (in SOA1) and once with C (SOA2), A is explained with Factor 1 (black) for the SOA1 sample and with Factor 2 (red) for the SOA 2 sample. Even increasing the number of factors does not create a "common" factor which contains only A. For this scenario, the different "source" for A (which lead to different compounds correlating with it) dominates the factor identification and not the fact that A, B, and C have the same volatility. Note that compound D which also does not change between SOA1 and SOA2 is separated into its own factor. Here the difference in volatility (from A, B, and C) is the driving force for the factor grouping.

In scenario Z, SOA3 and SOA4 each contain all 4 compounds. The concentration of A is the same in both types while the contribution of C is higher in SOA4 than in SOA3 and that of B is lower. The 3-factor solution for this scenario is depicted in Figure S 12. Again, we find two factors explaining the behaviour of the three compounds with the same volatility. But now factor 2 (red, dominated by A and C) has a considerable contribution to both SOA types. Figure S 13 shows how the thermograms of A are explained by the two factors. Similar to scenario X, we can interpret the factor grouping by changes in the processes/sources producing the compound A, B, and C. Factor 1 (black) stands for process 1 creating the majority of C and some A. Process 2 creates mostly A and B is explained by factor 2. Again factor 3 (containing D) is again differentiated by the different volatility of D. Integrating the factor thermogram profiles shows that the more volatile fraction of SOA4 is formed by process 2 while that the fraction of SOA3 with the same volatility is formed by both processes 1 and 2 (Figure S 14).

This Scenario Z is very similar to comparing e.g. samples from low- and mediumOC SOA. Many ions occur in both SOA types, but the ratios between them change. Many products in the oxidation of α-pinene can be formed via different pathways, but depending on the reaction path, they will correlate with different other products. The change in the oxidation field (increase of $[O_3]$ and [OH]) probably affected the HO_2/RO_2 chemistry which has a strong influence on e.g. highly oxygenated material (HOM) and dimer formation, i.e. we changed the ratio between reaction paths.

SI section 1.4:

1.4 PMF analysis of a dataset combining different SOA types

To study if the different SOA types are really as different as the factors identified in section 3.1 suggest or if this was artificially introduced by pre-grouping the data, we conduct a PMF analysis with the data grouped by sampling conditions. The dry, t = 4 h

set was chosen for detailed analysis as we did not want to introduce the added complication of aqueous phase chemistry and the dry lowOC sample at t = 0.25 h had a large contamination unique to that sample. In the following, we will refer to this as the "combined dataset". The analysis conducted with data pre-grouped by the SOA type will be labelled "pre-grouped".

The 8- and 13 factor solutions for the combined dataset are shown in Figure S 15 and Figure S 16. Based on the change in $Ratio_{exp}$ values and the residual time series, 8 was the minimum number of factors need to capture the thermograms of all 3 SOA types equally well. But to reach residuals as low as in the pre-grouped datasets, 13 factors are needed. Especially the lower T_{desorp} regions in the low- and highOC case and the high T_{desorp} part of the mediumOC sample are improved (Figure S 17). Note that with the same criteria applied in the section 2.3.3, we would not select the 8-factor solution as a "best" solution. There are no factors in the 8-factor solution which are unique to one SOA type. 4 factors (FV1, FV4, FV7, and FB/D1) occur in all SOA types explaining 80% of the signal of the mediumOC sample and 50% of the low- and highOC samples. The other 50% of the signal are explained with two factors each (lowOC: FV2 and FV5, highOC: FV3 and FV7) which also occur in the mediumOC sample.

The 8-solution suggests very strong similarities between the three SOA types with a gradual shift in composition with increasing oxidation. But this solution does not capture the detailed thermogram behaviour of single ions very well as the high residuals suggest (Figure S 18 for the example ion also discussed in sections 3.2 and 3.3). When this is improved in the 13-factors solution, the degree of similarity decreases. Here, 20% - 25% of the signal in each SOA type is explained by factors common to all SOA types (FD1, FB1, and FV1). There are some factors with significant contribution to two SOA types (e.g. FV2 and FV10 for low-/mediumOC or FV3, FV6 and FV11 for medium-/highOC).

To compare the factor mass spectra derived with the combined and the pre-grouped datasets, we use the spectral contrast angle, θ. θ is derived from the dot product of two mass spectra (Wan et al., 2002):

$$cos\theta = \frac{\sum_i a_i b_i}{\sqrt{\sum_i a_i^2 \cdot \sum_i b_i^2}}$$

where a_i and b_i are the intensities of ion i in mass spectrum 1 and mass spectrum 2. Two mass spectra are considered to be similar if θ is between 0° and 15°, somewhat similar but with important differences if θ is between 15° and 30°, and different with θ values >30° (Bougiatioti et al., 2014).

The results from the pairwise comparison of each factor identified in the pre-grouped datasets with all factors from the combined dataset are shown in Figure S 19. All V-type factors identified in the pre-grouped dataset have a (at least somewhat) similar counterpart in the combined dataset (e.g. LV4 and FV7, MV4 and FV8, HV2 and FV6). This shows that the missing similarities between factors identified in the pre-grouped dataset is not artificially induced by the pre-grouping but rather stems from the shifts in SOA composition with increasing oxidation. The changes in the groups of correlating ions will cause compounds that occur in all SOA types to be grouped into different factors as explained with the simplified dataset in SI section 1.3. The factors FV2, FV3, and FV4 show similarities to two factors within the corresponding SOA types. This suggests that either more factors are needed in the combined dataset to resolve the thermogram behaviour of the compounds represented by these factors, or that there was "factor-splitting" in the pre-grouped dataset (i.e. too many factors). Also, the combined

dataset uses only the information from the dry, t_{evap} = 4 h sample while the pre-grouped ones contain all 4 sampling types. Thus, behaviour unique to a different sample type cannot be correctly captured (e.g. LC1&2 or H-WET).

This case study shows that the same overall conclusions can be drawn by using pre-grouping the data according to the information of the sampling conditions (here the SOA type) or the combined dataset. With the combined dataset a higher number of factors (here at least 13) has to be chosen to cover all details in the dataset equally well. For ambient data a combined, dataset approach is favourable as limited information is available for any pre-grouping and such an extra step is not desirable. For a detailed study on e.g. particle phase processes with designed SOA types (as presented in this study), a pre-grouping can be beneficial to highlight the fine details hidden in the dataset.

Experimental Design

SI 1.1: Some experimental designs are unclear. Did the collection of the 0.25 hr isothermal evaporation sample start immediately after filling up after size selection? Was the t_0.25hr aerosol collected directly at the outlet of the DMA column, or was the aerosol drawn through the RTC first?

The t_{evap} = 0.25h sample was collected directly from the outlet of the Nano-DMAs and the residence time is the average time particles resided on the filter between their collection and the start of the desorption. The 15 min residence time for "fresh" particles and its consequences is explained in the last paragraph of SI section 1.1. We have included this information now in the short description in the main manuscript and modified the passage in SI section 1.1 to make this clearer:

Main text:

Note that the evaporation time of 0.25 h for the "fresh" sample does not stem from residence in the RTC but rather from the collection time on the filter (see SI section 1.1 for details). Due to this minimum evaporation time the FIGAERO-CIMS measurements will underestimate the contribution of volatile compounds in the particles as they leave the OFR.

SI section 1.1:

Two types of particles samples were collected with the FIGAERO-CIMS: "fresh" particles (labelled t_{evap} = 0.25h) were collected directly after size selection with a nano differential mobility analyser (NanoDMA, 80 nm electro mobility size) and "RTC" particles (labelled t_{evap} = 4h) which were left to evaporate at ~20 °C for 3 - 4 h in a residence time chamber (RTC) prior to collection on the FIGAERO filter.

Evaporation of aerosol already collected on the filter during the 15 minute collection period is likely to be significant for t_0.25hr samples, and should therefore be taken into account. It would be good to show, at least qualitatively, how much effects this has for different evaporation timescales.

The collection period was 30 min for the fresh samples. 15 min is the average time the particles reside on the filter before the desorption starts. From the isothermal evaporation experiments we know that between 4% (highOC, dry) and 32% (lowOC,

wet) of the particle volume evaporates in the first 15 min. This information was used when comparing the contribution of V-type factors in Figure 8. The x-axis position of the bars is the average VFR value from the isothermal evaporation

Considering the potential artifacts introduced by the use of a stainless RTC (as mentioned by the other referee), I was surprised that the authors did not attempt (or mention) isothermal evaporation directly over the FIGAERO filter, as has been done in some previous studies (e.g. Schobesberger et al. 2018). It seems to me a lost opportunity to monitor gas-phase changes that can corroborate particle-phase observations. I would like to see a comparison between isothermal evaporation RTC vs. FIGAERO filter results, at least under dry condition, that shows if there is any systematic biases introduced by the use of RTC.

Such a direct comparison of these two methods would indeed be very interesting. Please, note that our experiments were conducted in 2016 while the earliest publications about FIGAERO-filter evaporation studies came out in 2018 (D'Ambro et al., 2018). Later, we did discussed our results with scientist involved in the FIGAERO-filter evaporation studies. Direct comparisons of the methods are difficult as different FIGAERO and chamber design were used. However, qualitatively we observe very similar behaviour, namely the removal of the signal fraction at lower Tdesorp values leading to more shallow and broader single ion thermograms.

The original purpose of the experiments creating this data set was to provide reliable and direct measurements of isothermal evaporation as a base for detailed process modelling (Buchholz et al., 2019; Yli-Juuti et al., 2017). The particle size measurements during isothermal evaporation in the RTC is not biased by any assumptions about mass conservation/wall losses/filter collection issues. The FIGAERO-CIMS measurements were added to quantify chemical composition changes during this isothermal evaporation as the Aerosol Mass Spectrometer (AMS, Aerodyne Research Inc.) could not reliably detect the expected changes.

The potential artefacts of stainless-steel walls are mostly concerning reactions on those walls (e.g. peroxide decomposition as mentioned by reviewer #2) or increased uptake of oxygenated compounds from the gas phase. In our setup, all compounds that evaporate from the particles are considered lost to the walls and not interfering with the particles anymore. Tests with different aerosol loadings in the RTC showed no significant differences in particle evaporation. This confirms that the stainless-steel walls are very effective in taking up the evaporated compounds and there is no build-up of compounds in the gas phase. We are collecting and investigating the remaining particles after isothermal evaporation in the RTC and determine their composition. This composition is representative for the residual particles after isothermal evaporation independent on how many particles were lost to the walls and what happened to the evaporated vapours once they were taken up by the walls.

With the FIGAERO-filter evaporation method different types of possible artefacts have to be considered, e.g. differences in mass loading on the filter can shift T_{max} values considerably (SI material to Huang et al., 2018). These can be avoided with the RTC based approach presented here.

Minor comments

Figure S5: Were the labels for MV1 and MV2 switched? It is also surprising that the Tmax increases going from ELVOC, LVOC, to SVOC categories, if the labels are indeed correct.

Yes, the labels M1 and M2 were indeed switched in Figure S5. We corrected this. Note that the labels were correct in Figure 6 in the main manuscript.

Page 2. Line 5: The application of this technique to ambient data is not shown or discussed in the manuscript. This sentence should be removed.

We simply want to point out that the presented method is not restricted to lab data sets. We are currently studying the application of this method to an ambient data set which will be the content of a future publication.

Page 2. Line 6: What is meant by "physical source"?

We were referring to the typical "sources" identified with PMF analysis of e.g. AMS data. There factors are interpreted as organic aerosol (OA) types such as hydrocarbon-like (HOA) or oxygenated OA (OOA). Another way of interpretation is linking the time series of factors to other measurements identifying the process forming the OA (e.g. traffic emissions). We clarified this in the text:

There, it adds the information about particle volatility to that about the sources (such as biomass burning or oxidation of different precursors) or the type (e.g. hydrocarbon-like (HOA) or oxygenated organic aerosol (OOA)) of the organic aerosol particles which could also be obtained by PMF analysis of the mass spectra data integrated for each thermogram scan.

Page 4. Line 7-9: Operational details of the DMA column should be mentioned here.

We prefer to keep the description of the setup as brief as possible as it was already described elsewhere. The details for Nano-DMA operation are now given in SI section 1.1.

The NanoDMA was operated with an open loop sheath flow (10 L min^{-1}, (dry): 8 L min^{-1} (wet)) which together with the extremely short residence time inside the NanoDMA ($\leq$ 0.3 s) limited the diffusion of gaseous compounds into the selected sample flow (1 L min^{-1}).

Page 4. Line 9-11: Potential artifacts related to the use of stateliness steel chamber, e.g. peroxide decomposition, should be mentioned.

The system is not operated in a partitioning equilibrium, but rather so that all evaporating vapours are quickly lost to the walls as shown in (Yli-Juuti et al., 2017). Thus, it does not matter if a peroxide that evaporated from a particle decomposes on the RTC wall as long as the decomposition products are not released back into the gas phase and interact with the particles.

Page 7. Line 2-3: What is the reason for using the absolute value instead of the squared value?

When using the squared values with our data, the sum of $Var_{explained}$ and $Var_{unexplained}$ was not equal to Var_{total} but much smaller for PMF solutions with low factor number and larger for solutions with higher factor numbers. This led to $Ratio_{exp}$ >1 which were not meaningful in this context. Also, if the calculation was performed in the other dimension, i.e., calculating the variance with respect to the average value for each observation j instead of the average for each ion i, the values for $Var_{explained}$ / Var_{total} changed.

When using the absolute distances instead of the quadratic this behaviour changed and $Var_{explained} + Var_{unexplained} \approx Var_{total}$. Thus, we decided to use this metric as a compromise.

Page 9, Line 27-29: Please remove the “great”s.

Text was changed.

Page 10, Line 4: Ulbrich et al., 2009 has already shown that the change in Q/Qexp with respect to the number of factor is a more reliable indicator than Q/Qexp. This is mentioned later in this manuscript, but should perhaps be moved up to this section here.

Yes, the reviewer is correct. We have actually pointed this out in our original submission (page 10, line 17):

“However, the shape of the Q/Q_{exp} vs number of factors curve can be used to judge the impact of introducing another factor, i.e., a large change in Q/Q_{exp} suggests the new factor explains a large fraction of the variability in the data (Ulbrich et al., 2009).”

Page 10, Line 13-16: Maybe a quotient could be defined here, such as the incremental increase in ion behaviors well-captured (what is the criteria for "well-captured"?) vs. number of factors chosen. What is correlation of the two for the PMF solutions obtained here?

One difficult issue is the fact that the typical parameters to judge the quality of a PMF solution (like Q/Qexp or explained variance) did not provide insights regarding these specific ions and if their characteristic behaviour was captured. As these metrics are all summed over all ions and/or observations they are apparently not sensitive. It was in each case only a few ions where the behaviour was obviously not captured. These ions were all classified as “strong” (i.e., good signal-to-noise ratio). But compared to the large number of other ions, they seem to not have a big enough impact on things like Q/Qexp or explained variance. The most robust way was to inspect the residuals as time series and mass spectra to identify time periods and ions that were not treated adequately.

Page 11, Line 17-19: Table 1 would suggest that background ions were dominated by organic residues instead of fluorinated compounds. Which is the case here?

Fluorinated compounds were identified in the samples but accounted for less than 1% of the total signal. The average F content for V-type factors was < 0.01 and higher for B-, C-, and D-type factors (0.01 – 0.05). The small increase shows that there was

a contribution of “Teflon” compounds to the background, but the majority of the B factor compounds are indeed residual compounds and/or contaminations during sampling.

As the contribution of fluorine to the average compositions was so small, it was omitted in Table 1 in the manuscript.

Figures

The figures are the same as were added to the SI material. Thus, we use the same labels and numbering here.

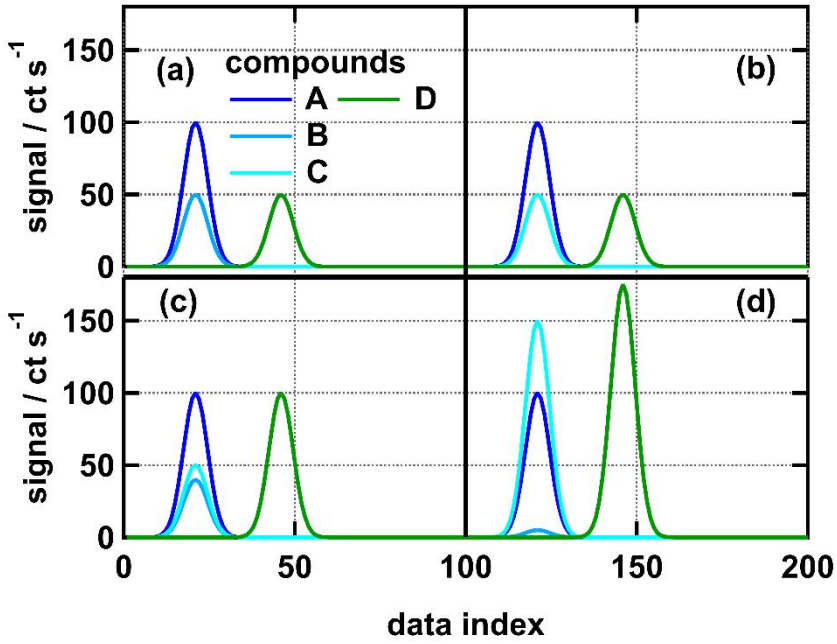

Figure S 10: Artificial thermogram data for four SOA types. (a) SOA1, (b) SOA2, (c) SOA3, (d) SOA4. SOA1 and SOA2 are combined in one data set for scenario X and so are SOA3 and SOA4 for scenario Z. Note that the thermograms are plotted vs data index. Compounds A, B, and C have the same T_{max} values in all SOA types.

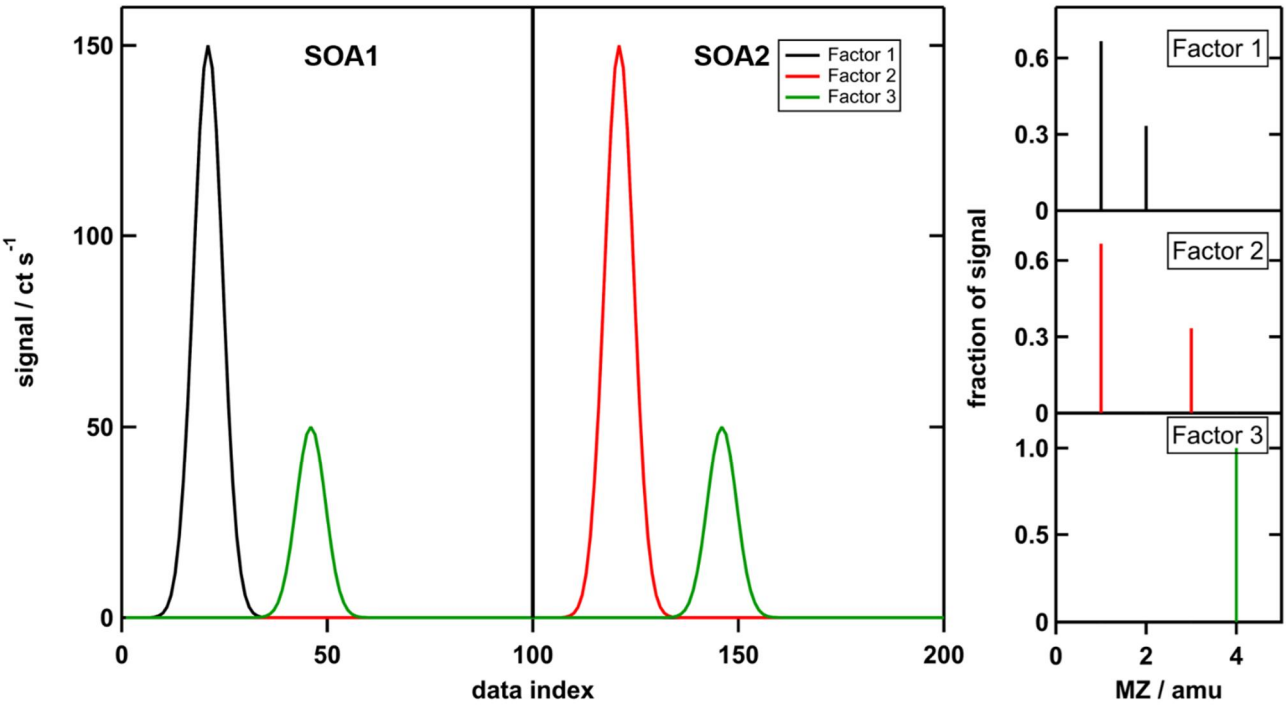

Figure S 11: Factor thermogram profiles (left) and factor mass spectra (right) for the 3-factor solution for scenario X. For plotting, the compounds A, B, C, D are assigned the nominal MZ values 1, 2, 3, 4 respectively.

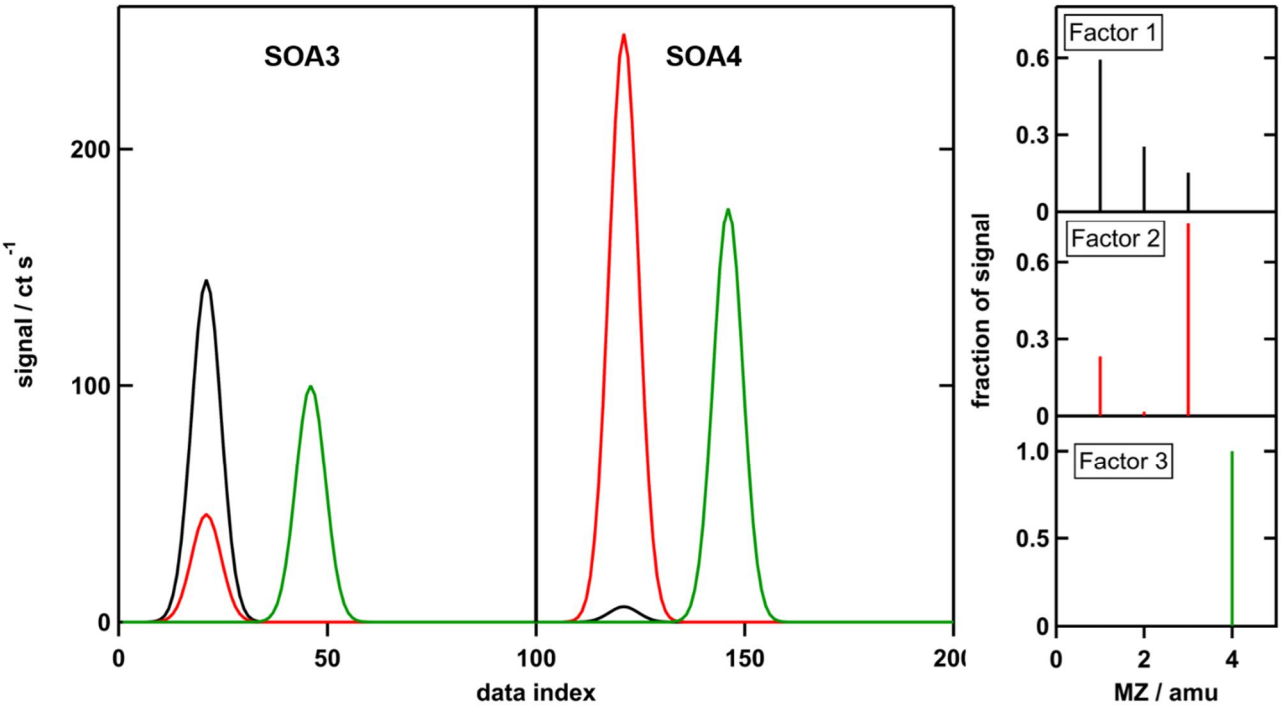

Figure S 12: Factor thermogram profiles (left) and factor mass spectra (right) for the 3-factor solution for scenario Z. For plotting, the compounds A, B, C, D are assigned the nominal MZ values 1, 2, 3, 4 respectively.

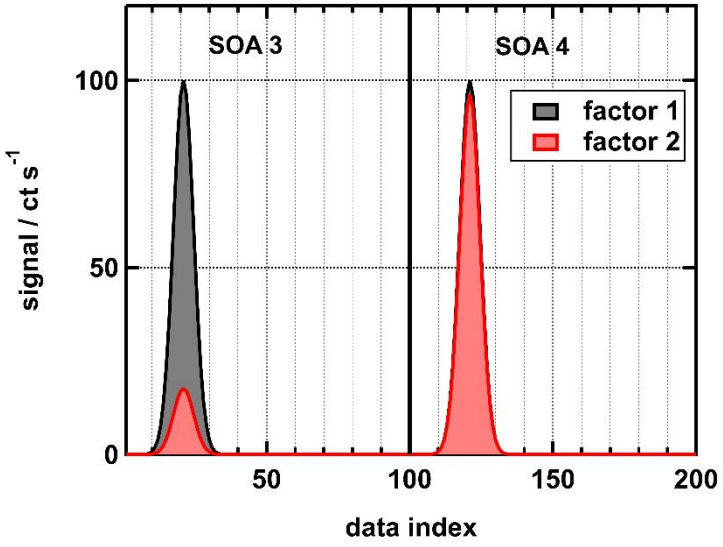

320

Figure S 13: Factor thermogram for compound A in scenario Z.

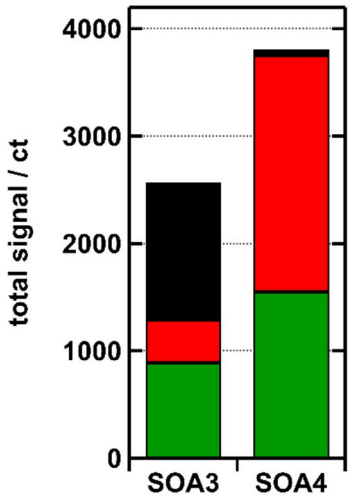

Figure S 14: Absolute contribution of factors to the signal of SOA3 and SOA4 in the scenario Z. Black: factor 1, red: factor 2, green: factor 3.

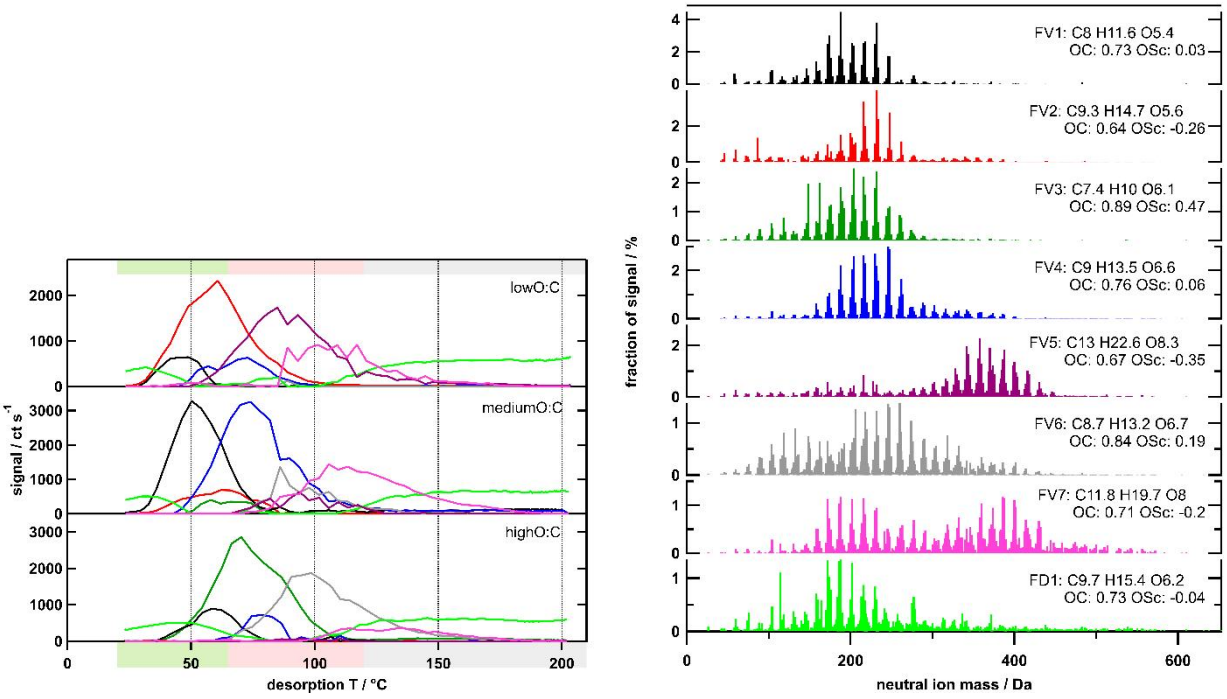

Figure S 15: Temperature profiles (left) and factor mass spectra (right) for the 8-factor solution the combined dataset for dry, t = 4 h samples. Each factor mass spectrum is normalised. The colour code is the same for both panels. Background colour in the left panel indicates volatility classification derived from T_{max}-C* calibrations (green: SVOC, red: LVOC, grey: ELVOC).

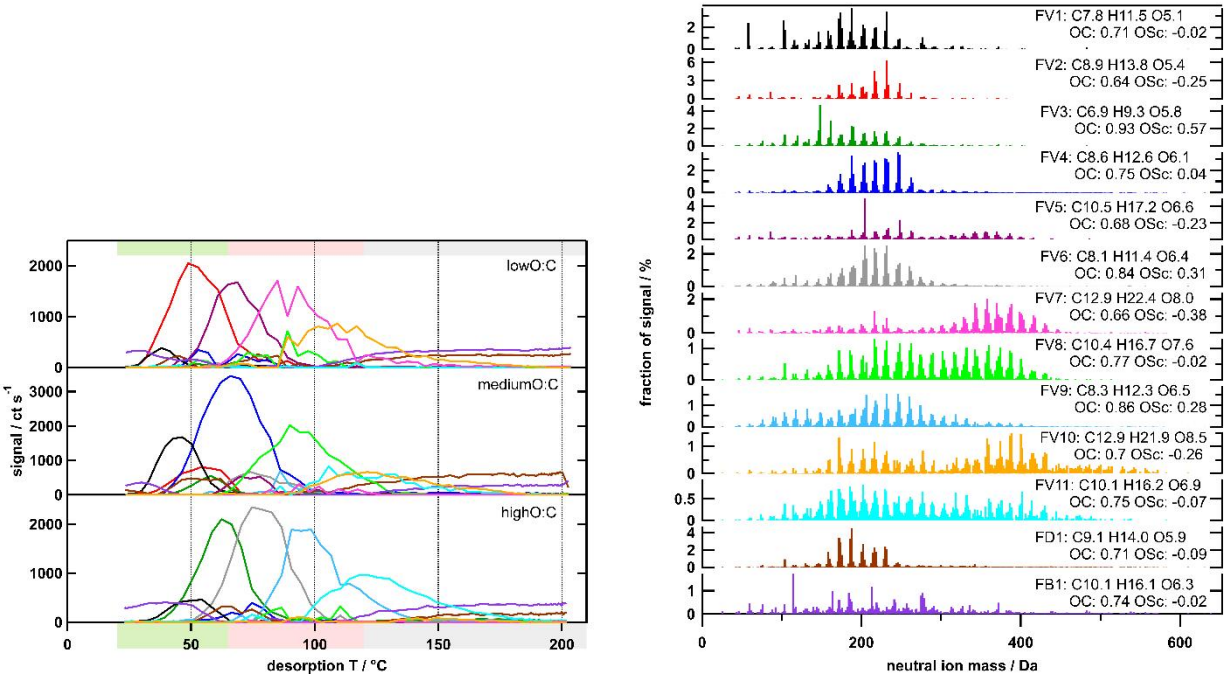

Figure S 16 Temperature profiles (left) and factor mass spectra (right) for the 8-factor solution the combined dataset for dry, t = 4 h samples. Each factor mass spectrum is normalised. The colour code is the same for both panels. Background colour in the left panel indicates volatility classification derived from Tmax-C* calibrations (green: SVOC, red: LVOC, grey: ELVOC).

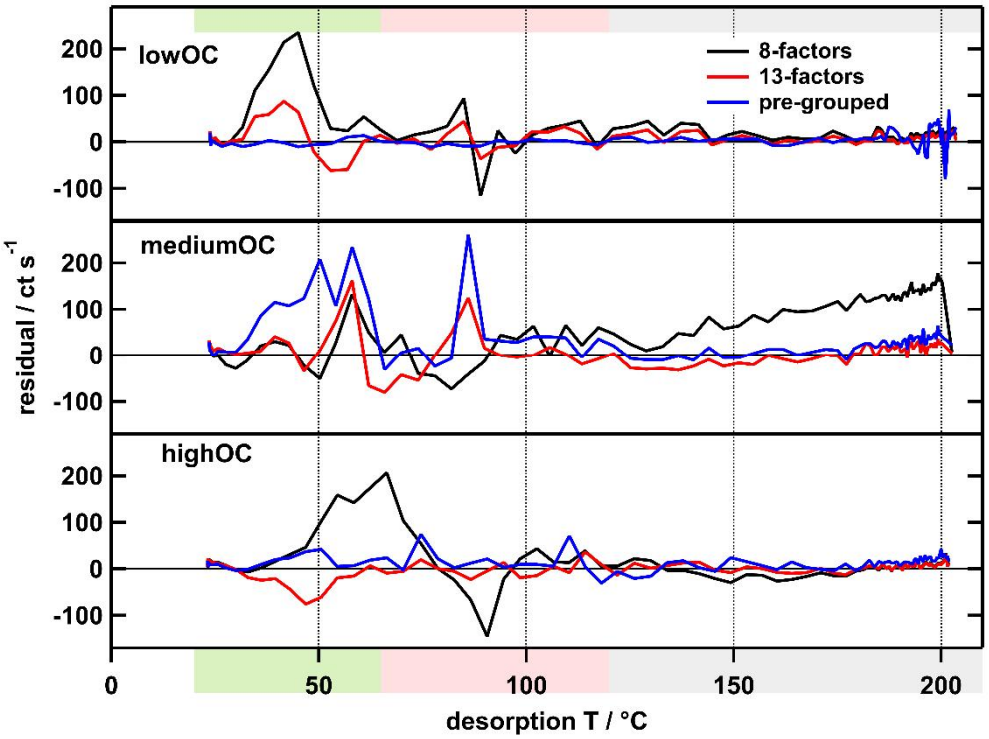

Figure S 17 Time series of residuals for the 8-(black) and 13- factor (red) solutions for the combined dataset and the corresponding pre-grouped datasets (blue).

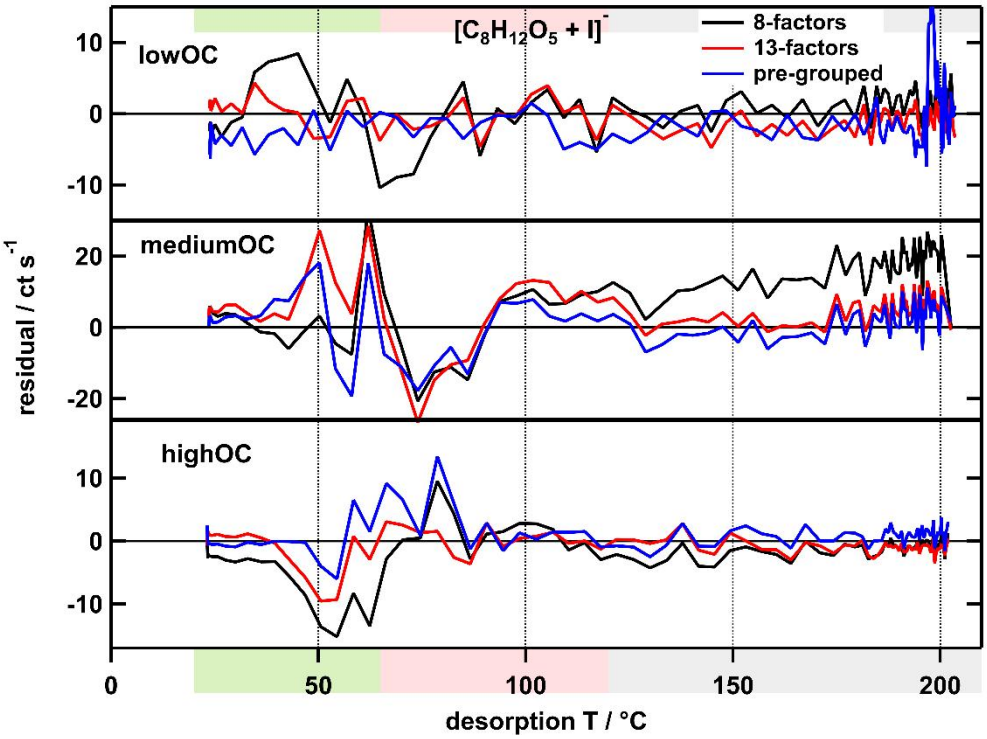

Figure S18: Time series of residuals of the ion $[C_8H_{12}O_5 + I]^-$ for the 8-(black) and 13- factor (red) solutions for the combined dataset and the corresponding pre-grouped datasets (blue).

340

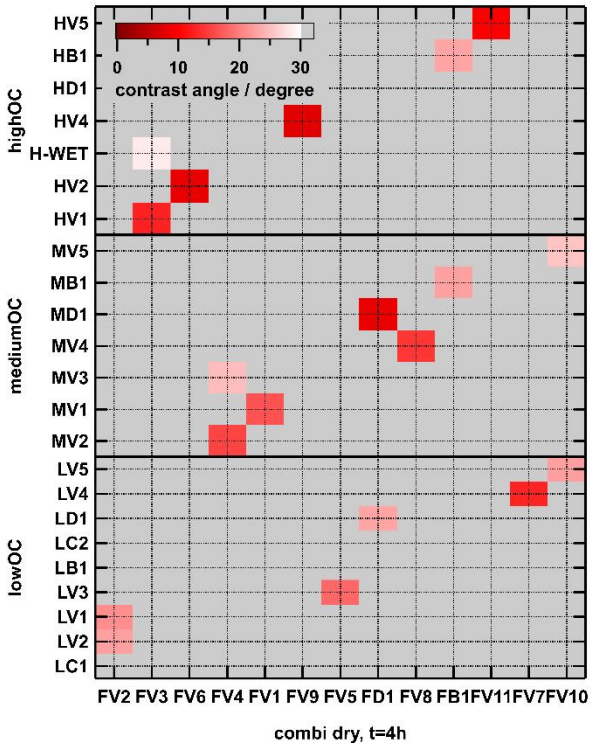

Figure S 19: Contrast angle plot comparing the factor mass spectra from the separate PMF analysis of each SOA type with those from the combined analysis with 13 factors. Grey areas indicate no similarity (contrast angle > 30°) while shapes of red indicate decreasing degree of similarity from dark to light.

References

Bougiatioti, A., Stavroulas, I., Kostenidou, E., Zarmpas, P., Theodosi, C., Kouvarakis, G., Canonaco, F., Prévôt, A.S.H., Nenes, A., Pandis, S.N., Mihalopoulos, N., 2014. Processing of biomass-burning aerosol in the eastern Mediterranean during summertime. Atmos. Chem. Phys. 14, 4793–4807. https://doi.org/10.5194/acp-14-4793-2014

Buchholz, A., Lambe, A.T., Ylisirniö, A., Li, Z., Tikkanen, O.-P., Faiola, C., Kari, E., Hao, L., Luoma, O., Huang, W., Mohr, C., Worsnop, D.R., Nizkorodov, S.A., Yli-Juuti, T., Schobesberger, S., Virtanen, A., 2019. Insights into the O:C dependent mechanisms controlling the evaporation of a-pinene secondary organic aerosol particles. Atmos. Chem. Phys. Discuss. 1–21. https://doi.org/10.5194/acp-2018-1305

D'Ambro, E.L., Schobesberger, S., Zaveri, R.A., Shilling, J.E., Lee, B.H., Lopez-Hilfiker, F.D., Mohr, C., Thornton, J.A., 2018. Isothermal Evaporation of α-Pinene Ozonolysis SOA: Volatility, Phase State, and Oligomeric Composition. ACS Earth Sp. Chem. 2, 1058–1067. https://doi.org/10.1021/acsearthspacechem.8b00084

Huang, W., Saathoff, H., Pajunoja, A., Shen, X., Naumann, K.-H., Wagner, R., Virtanen, A., Leisner, T., Mohr, C., 2018. α -Pinene secondary organic aerosol at low temperature: chemical composition and implications for particle viscosity. Atmos. Chem. Phys. 18, 2883–2898. https://doi.org/10.5194/acp-18-2883-2018

Ulbrich, I.M., Canagaratna, M.R., Zhang, Q., Worsnop, D.R., Jimenez, J.L., 2009. Interpretation of organic components from Positive Matrix Factorization of aerosol mass spectrometric data. Atmos. Chem. Phys. 9, 2891–2918. https://doi.org/10.5194/acp-9-2891-2009

Wan, K.X., Vidavsky, I., Gross, M.L., 2002. Comparing similar spectra: From similarity index to spectral contrast angle. J. Am. Soc. Mass Spectrom. 13, 85–88. https://doi.org/10.1016/S1044-0305(01)00327-0

Yli-Juuti, T., Pajunoja, A., Tikkanen, O.P., Buchholz, A., Faiola, C., Väisänen, O., Hao, L., Kari, E., Peräkylä, O., Garmash, O., Shiraiwa, M., Ehn, M., Lehtinen, K., Virtanen, A., 2017. Factors controlling the evaporation of secondary organic aerosol from a-pinene ozonolysis. Geophys. Res. Lett. 44, 2562–2570. https://doi.org/10.1002/2016GL072364